Materials Science-Poland, 37(2), 2019, pp. 238-243
http://www.materialsscience.pwr.wroc.pl/
DOI: 10.2478/msp-2019-0018

Structural and thermal properties of Zn-containing magnesium aluminate spinels obtained by wet chemical method

OMER KAYGILI[1,*], NIYAZI BULUT[1], TANKUT ATES[1], ISMAIL ERCAN[2], SULEYMAN KOYTEPE[3], TURGAY SECKIN[3], CENGIZ TATAR[1], BAYRAM GUNDUZ[4], HANIFI KEBIROGLU[1]

[1]Department of Physics, Faculty of Science, Firat University, 23119, Elazig, Turkey
[2]Department of Biophysics, Institute for Research and Medical Consultations, Imam Abdulrahman Bin Faisal University, 34441, Dammam, Saudi Arabia
[3]Department of Chemistry, Faculty of Arts & Science, Inonu University, 44280, Malatya, Turkey
[4]Department of Science Education, Faculty of Education, Mus Alparslan University, 49250, Mus, Turkey

In the present study, the dopant effect of Zn on the crystal structure, thermal properties and morphology of magnesium aluminate ($MgAl_2O_4$) spinel (MAS) structure was investigated. A pure and two Zn-containing MASs (e.g. $MgAl_{1.93}Zn_{0.07}O_4$ and $MgAl_{1.86}Zn_{0.14}O_4$) were synthesized for this purpose via a wet chemical method, and the as-prepared samples were characterized by X-ray diffraction (XRD), Fourier transform infrared (FT-IR) spectroscopy, differential thermal analysis (DTA), thermogravimetric analysis (TGA), scanning electron microscopy (SEM) and energy dispersive X-ray (EDX) spectroscopy techniques. It was found that the crystal structure, thermal properties and morphology of the MAS system change with the increase in the amount of Zn. MgO phase formation was observed. The values of the lattice parameter, unit cell volume and crystallite size increased, and the crystallinity percentage decreased. The morphology was also affected by adding of Zn.

Keywords: *spinel; wet chemical method; crystal structure; thermal properties; morphology*

1. Introduction

Spinels with the chemical formula of AB_2O_4, where A and B are cations in the tetrahedral and octahedral sites, respectively are a class of minerals [1, 2]. Magnesium aluminate ($MgAl_2O_4$) spinel (MAS), which is a member of this class, is a very attractive material used for a long time in various industrial applications due to its excellent structural properties including, high melting point, low dielectric constant, high refractoriness, excellent resistance to chemical attack, high electrical resistivity, low thermal conductivity and high resistance to radiation damage [3–12].

There is a great number of reports on the MAS system. The optical properties of MASs implanted with He ions were studied by Gritsyna et al. [13]. Izumi et al. [14] investigated the optical response and electronic structure of Zn-doped MAS single crystals grown by a floating-zone method. The effect of Zn substitution in the place of Mg in MASs on microwave dielectric properties was reported by Zheng et al. [15]. The effects of co-dopants of Co and Zn replacing Mg on the physical properties of semiconducting MAS prepared via solution combustion synthesis assisted by microwave irradiation, were studied by Iqbal et al. [16]. The photocatalytic properties of MASs synthesized by sol-gel auto combustion method using various fuels (e.g. oxalic acid, urea, and citric acid) at different temperatures were investigated by Nassar et al. [17]. The formation of a thin MAS layer at the Al/MgO interface was reported by Yang et al. [18]. A detailed study on the effect of average grain size on the static and dynamic mechanical properties of transparent polycrystalline MAS was performed by Sokol et al. [19]. Characterizations of ZnO containing MASs produced by solid oxide reactions

*E-mail: okaygili@firat.edu.tr

of calcined magnesia and calcined alumina were made by Ghosh et al. [20]. The optical properties of transition metal (Ti, Mn and V) doped MASs were investigated by Hanamura et al. [21]. The effect of transition metals of Ti and Mn on the optical properties of MAS grown by the micro-pulling-down method was reported by Jounini et al. [22]. Zhang et al. [23] produced the TiAlN/$MgAl_2O_4$ nanomultilayers with different $MgAl_2O_4$ layer thickness and reported that crystallization of $MgAl_2O_4$ layers plays a key role in the strengthening-toughening behavior of these nanomultilayers.

In this work, we aimed to investigate the effect of Zn adding on the crystal structure, phase composition, thermal properties and morphology of MAS. In this context, three $MgAl_{2-x}Zn_xO_4$, spinels, where x was chosen as 0, 0.07 and 0.14, were prepared using a wet chemical synthesis, and the as-obtained MASs were characterized via X-ray diffraction, Fourier transform infrared (FT-IR) spectroscopy, differential thermal analysis (DTA), thermogravimetric analysis (TGA), scanning electron microscopy (SEM) and energy dispersive X-ray (EDX) spectroscopy.

2. Materials and method

The preparation of $MgAl_2O_4$, $MgAl_{1.93}Zn_{0.07}O_4$ and $MgAl_{1.86}Zn_{0.14}O_4$ samples was performed using the following steps. The chemicals of magnesium nitrate hexahydrate (MN, $Mg(NO_3)_2{\cdot}6H_2O$), aluminum nitrate nonahydrate (AN, $Al(NO_3)_3{\cdot}9H_2O$) and zinc nitrate hexahydrate (ZN, $Zn(NO_3)_2{\cdot}6H_2O$) were purchased from Sigma-Aldrich and used as received. Appropriate amounts of these chemicals were dissolved in distilled water in the order of MN, AN and ZN for each sample. The as-prepared solutions were mixed in a magnetic stirrer at 90 °C for 1 h. The solutions were dried in an oven at 130 °C for 21 h, and then heated in an electric furnace at 950 °C for 2 h in order to eliminate the residues such as nitrates and carbonates. In this way, the pure and Zn-assisted MASs were obtained.

XRD analyses of the powdered samples were performed using a Rigaku diffractometer, RadB-DMAX II model in the 2θ range from 10 to 80° with a step size of 0.02° using CuKα (0.15406 nm) radiation filtered with Ni. Using the KBr pellet method, Fourier transform infrared (FT-IR) spectra were measured using a PerkinElmer Spectrum One spectrometer with a spectral resolution of 4 cm^{-1} in the wavenumber range of 400 cm^{-1} to 4000 cm^{-1}. A Shimadzu DTA 50 was used to investigate thermal behavior of the as-synthesized MASs, and this measurement was carried out by heating 10 mg of each sample in a Pt crucible in the temperature range of 25 °C to 1000 °C at a heating rate of 10 °C·min^{-1}. Thermogravimetric analysis experiments were performed on a Shimadzu TGA 50 thermal analyzer. The morphology investigation and elemental analysis of the as-prepared samples were performed using a scanning electron microscope (SEM, LEO EVO 40xVP) equipped with an energy dispersive X-ray (EDX, Röntech xflash) spectrometer. The SEM images were taken with an accelerating voltage of 20 kV and at magnification of ×2500 for each sample.

3. Results and discussion

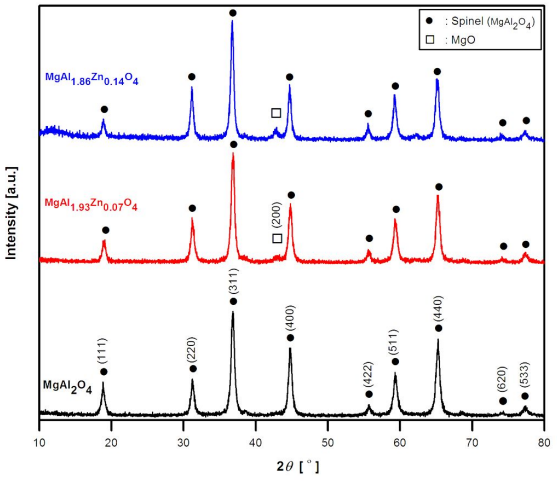

Fig. 1. XRD patterns of as-prepared MASs.

Fig. 1 shows the X-ray diffraction (XRD) patterns of pure and Zn-containing MASs. The pure MAS is composed of a single phase of $MgAl_2O_4$ (JCPDS PDF# 21-1152) with a cubic crystal structure, and no impurity has been detected in this sample. For Zn-containing samples, besides

the major phase of $MgAl_2O_4$ (JCPDS PDF# 21-1152), the formation of secondary phase of MgO (JCPDS PDF# 79-0612) having cubic crystal structure is observed. While the diffraction peaks of (1 1 1), (2 2 0), (3 1 1), (4 0 0), (4 2 2), (5 1 1), (4 4 0), (6 2 0) and (5 3 3) planes belonging to $MgAl_2O_4$ phase have been detected in all the samples, the peak of (2 0 0) plane corresponding to MgO phase is observed only for Zn-doped MASs. The crystal structure has not changed despite the formation of the new phase. Additionally, the amount of MgO phase increased with adding of Zn, namely, MgO content was detected to be 3.8 % and 5.6 % for $MgAl_{1.93}Zn_{0.07}O_4$ and $MgAl_{1.86}Zn_{0.14}O_4$ samples, respectively.

All the XRD results concerning the crystallite size D, crystallinity percentage X_C, lattice parameter a and unit cell volume V for each sample are listed in Table 1. The crystallite sizes were calculated for both the most intense peak of (3 1 1) plane as D_{311} and all the diffraction peaks of MAS structure as an average value D_{avg} for each sample, using following Scherrer equation 1:

$$D = \frac{0.9\lambda}{\beta \cos\theta} \tag{1}$$

where λ is the wavelength of incident X-rays wavelength (0.15406 nm for CuKα radiation), β is the full width at half maximum (FWHM), and θ is the Bragg angle.

Just as in the calculation of the crystallite size, the average value of lattice parameter (a = b = c) was computed for each sample using the following relation [24]:

$$a = d\sqrt{h^2 + k^2 + l^2} \tag{2}$$

where h, k, l are Miller indices, and d is the interplanar spacing of the crystal. The unit cell volume of the samples with a cubic crystal structure was evaluated using the following relation [24]:

$$V = a^3 \tag{3}$$

Calculation of the crystallinity percentage X_C % can be found in the literature [25].

As can be seen from the results given in Table 1, the crystallite size increases with increasing amount of Zn for both values, D_{311} and D_{avg}, whereas the D_{MgO} value calculated for the secondary phase of MgO decreases. Depending on this increase, the lattice parameter also increases with the addition of Zn, and a gradual expansion in the unit cell volume is observed. These increase may be explained as follows: The ionic radius of Zn^{2+} (0.074 nm) is greater than that of Mg^{2+} (0.065 nm) [26]. Due to this difference, the increase in the D, a and V values can be expected if Mg ions are replaced by Zn ions. The calculated values of the lattice parameter and crystallite size obtained in this study are in a very good agreement with the results reported by Saberi et al. [27], and Sanjabi et al. [28]. The crystallinity percentage decreases with increasing Zn content, and the presence of Zn ions in the MAS structure also causes MgO phase formation as mentioned before. According to the results reported by Deraz et al. [29], with the increase in magnesia (MgO) content in spinel structure, the crystallinity decreases, and in this regard, our finding is in a very good harmony with the literature. Both these findings and other ones given below also support the result that the composition of the spinel affects its properties [30].

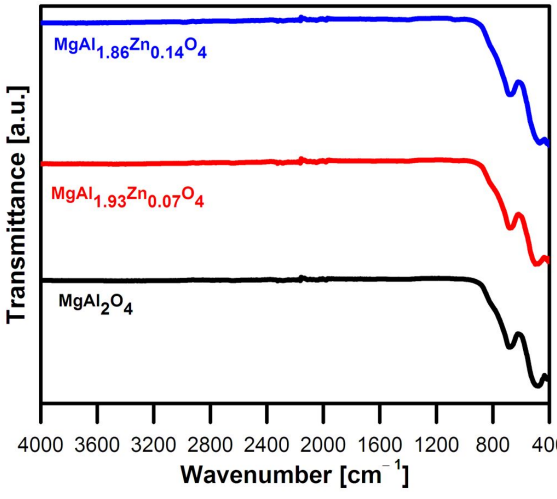

Fig. 2. FT-IR spectra of the as-synthesized MAS samples.

Fig. 2 shows the FT-IR spectra of the MAS samples. Two bands observed at about 481 cm^{-1} and 684 cm^{-1} are associated with the characteristic vibrations of metal-oxygen-metal bond belonging to

Table 1. The detailed XRD analysis report for the pure and Zn-containing MAS samples.

Sample	Phase composition [%]		D_{avg}	D_{311}	D_{MgO}	X_C	a	V
	$MgAl_2O_4$	MgO	[nm]	[nm]	[nm]	[%]	[nm]	[nm^3]
$MgAl_2O_4$ (JCPDS# 21-1152)	100.0	–	–	–	–	–	0.8083	0.5281
$MgAl_2O4$	100.0	–	14.77	15.20	–	99.1	0.8089	0.5293
$MgAl_{1.93}Zn_{0.07}O4$	96.2	3.8	15.37	16.30	23.10	95.7	0.8097	0.5308
$MgAl_{1.86}Zn_{0.14}O4$	94.4	5.6	16.60	16.72	10.51	93.5	0.8106	0.5326

Mg and Al elements, indicating $MgAl_2O_4$ formation [28, 31, 32]. While the band at 684 cm^{-1} observed for the pure MAS shifts to the wavenumber value of 680 cm^{-1} for both Zn-containing MASs, the other band detected at 481 cm^{-1} shifts to 479 cm^{-1} and to 472 cm^{-1} with increasing Zn content.

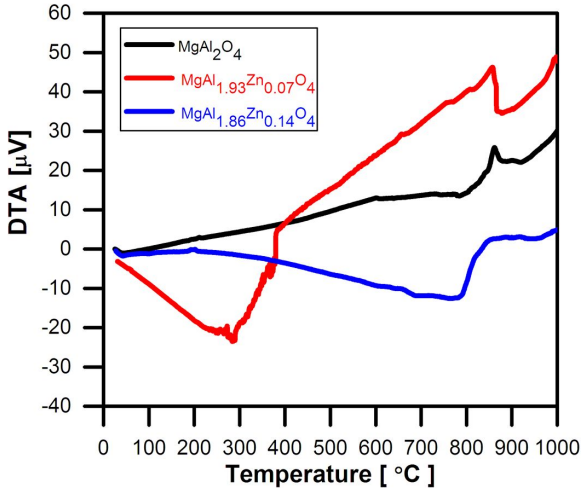

Fig. 3. DTA curves of the samples at the temperature range of 25 °C to 1000 °C.

The DTA curves of the as-synthesized MASs are plotted in Fig. 3. The wide endothermic peak centered at about 300 °C for $MgAl_{1.93}Zn_{0.07}O_4$ is associated to the removal of the adsorbed water in the sample [28, 33, 34]. Similar thermal behavior was reported by Gusmano et al. [35] for the MAS produced by thermal decomposition of co-precipitated hydroxides. An exothermic peak related to the formation of magnesium aluminate spinel structure [36] is observed at 862 °C, 857 °C and 851 °C for $MgAl_2O_4$, $MgAl_{1.93}Zn_{0.07}O_4$ and $MgAl_{1.86}Zn_{0.14}O_4$, respectively. The position of this peak shifts gradually from 862 °C to 851 °C with increasing Zn content. Additionally, as can be seen from Fig. 3, the sharpness of this peak decreases with adding of Zn. This decrease in the sharpness can be related to the decrease in the crystallinity of the samples, that is the crystallinity decreases with the addition of Zn. This finding supports the XRD results.

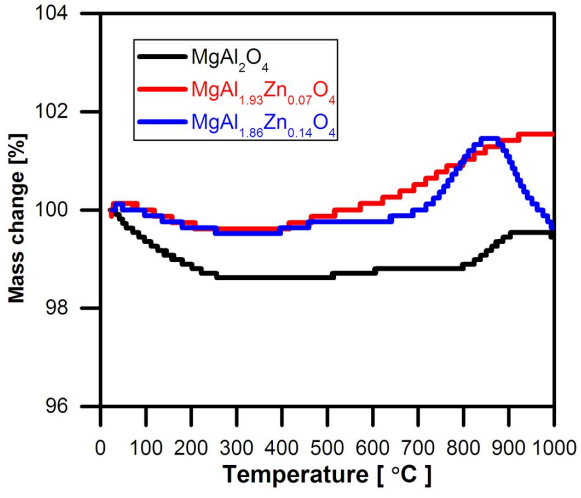

Fig. 4. TGA curves of the MAS samples.

Fig. 4 presents the TGA plots of the samples in the temperature range from 25 °C to 1000 °C. Similarly, there is a mass loss up to a certain temperature for all the samples, and then a mass gain is observed. The mass losses of 1.38 %, 0.38 % and 0.48 % up to the temperature of 511 °C, 416 °C and 396 °C have been detected for $MgAl_2O_4$, $MgAl_{1.93}Zn_{0.07}O_4$ and $MgAl_{1.86}Zn_{0.14}O_4$, respectively. It is seen that this limit value decreases in the temperature range of 511 °C to 396 °C with increasing Zn content. The mass gain starts after these temperatures and continues up to

903 °C, 922 °C and 839 °C for $MgAl_2O_4$, $MgAl_{1.93}Zn_{0.07}O_4$ and $MgAl_{1.86}Zn_{0.14}O_4$, respectively. Once 1000 °C is reached, there is a mass gain of 1.54 % for $MgAl_{1.93}Zn_{0.07}O_4$, while the mass loss of 0.46 % is detected for $MgAl_2O_4$. When the mass change of the sample with the highest Zn content ($MgAl_{1.86}Zn_{0.14}O_4$) is examined, it can be seen that a maximum mass gain of 1.45 % at the temperature of 858 °C is observed and then, unlike in the other two samples, an extra mass loss of 0.36 % is seen at 1000 °C. All the TGA curves are in a very good agreement with the reported one by Alvar et al. [37]. Although the mass change for all the samples is not remarkable, it can be seen that Zn content significantly affects the mass change in the MAS.

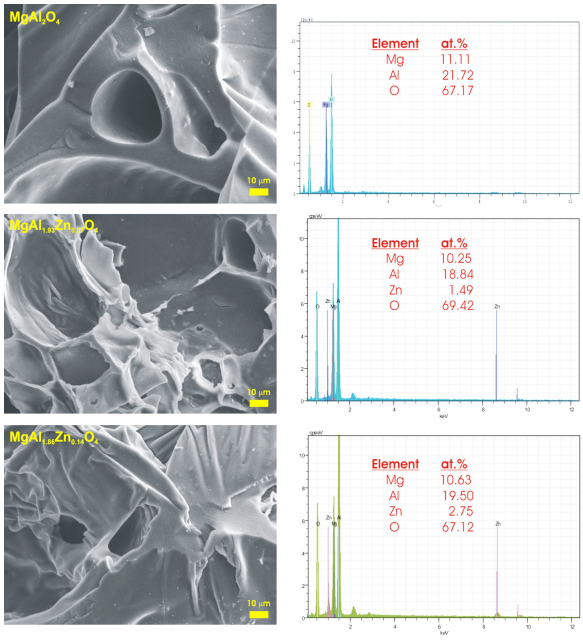

Fig. 5. SEM micrographs and EDX analysis reports for each sample.

The SEM micrographs, EDX spectra and elemental compositions of the MAS samples are given in Fig. 5. All the samples exhibit a dense and compact morphology. With increasing Zn content, the molar ratios of Al/Mg and (Al + Zn)/Mg for the pure and Zn-containing MAS samples were found to be 1.96, 1.98 and 2.09, and these values are very close to the stoichiometric ratio of 2.00, supporting magnesium aluminate spinel formation for each sample. For Zn-doped samples, the EDX analysis results confirm the introduction of Zn to the MAS structure, and as expected, the detected Zn content increases with increasing Zn amount.

4. Conclusions

A pure and two Zn-containing magnesium aluminate spinel (MAS) samples were successfully produced using a wet chemical synthesis at 950 °C. We can conclude that the addition of Zn into the MAS structure significantly affects all the investigated properties. The FT-IR, SEM and DTA results, as well as the XRD analysis, confirm the formation of MAS structure for all the samples. The crystallinity percentage decreases dramatically from 99.1 to 93.5, whereas the lattice parameter, MgO phase content and crystallite size increase gradually from 0.8089 nm to 0.8106 nm, from 0 wt.% to 5.6 wt.% and from ~15 nm to 17 nm, respectively, with increasing amount of Zn. For all the samples, the mass change in the temperature range from 25 °C to 1000 °C is less than or equal to 1.54 %. All the samples have a dense and compact morphology. Zn ions replacing those of Mg, affect the crystal structure, phase composition, thermal properties and morphology of the MAS samples.

Acknowledgements

This work was supported by Management Unit of Scientific Research projects of Firat University (FÜBAP) (Project Numbers: FF.15.03, FF.18.16, and FF.18.20).

References

[1] LIU M., RONG Z., MALIK R., CANEPA P., JAIN A., CEDER G., PERSSON K.A., *Energy Environ. Sci.*, 8 (2015), 964.
[2] LI N., DUAN X., YU F., JIANG H., *Vacuum*, 142 (2017), 1.
[3] GANESH I., *Int. Mater. Rev.*, 58 (2013), 63.
[4] SINHAMAHAPATRA S., SHAMIM M., TRIPATHI H.S., GHOSH A., DANA K., *Ceram. Int.*, 42 (2016), 9204.
[5] SARKAR R., SAHOO S., *Ceram. Int.*, 40 (2014), 719.
[6] NAKHOWONG R., KIENNORK S., WONGWANWATTANA P., SEETAWAN T., CHUEACHOT R., *Mater. Lett.*, 220 (2018), 234.
[7] MOHAN S.K., SARKAR R., *Mater. Design*, 110 (2016), 145.
[8] TANG C., ZHAI Z., LI X., SUN L., BAI W., *J. Taiwan Inst. Chem. E.*, 58 (2016), 97.

[9] OROSCO P., BARBOSA L., RUIZ M.D.C., *Mater. Res. Bull.*, 59 (2014), 337.
[10] LIU J., WANG Z., WANG X., LIU H., MA Y., *Ceram. Int.*, 44 (2018), 7416.
[11] CUI F.Y., KUNDU A., KRAUSE A, HARMER M.P., VINCI R.P., *Acta Mater.*, 148 (2018), 320.
[12] HABIBI N., WANG Y., ARANDIYAN H., REZAEI M., *Adv. Powd. Technol.*, 28 (2017), 1249.
[13] GRITSYNA V.T., AFANASYEV-CHARKIN I.V., KAZARINOV Y.G., SICKAFUS K.E., *Vacuum*, 81 (2006), 174.
[14] IZUMI K., MIZOKAWA T., HANAMURA E., *J. Appl. Phys.*, 102 (2007), 053109.
[15] ZHENG C.W., WU S.Y., CHEN X.M., SONG K.X., *J. Am. Ceram. Soc.*, 90 (2007), 1483.
[16] IQBAL M.J., ISMAIL B., RENTENBERGER C., IPSE H., *Mater. Res. Bull.*, 46 (2011), 2271.
[17] NASSAR M.Y., AHMED I.S., SAMIR I., *Spectrochim. Acta A*, 131 (2014), 329.
[18] YANG L., XIA M., BABU N.H., LI J., *Mater. Trans.*, 56 (2015), 277.
[19] SOKOL M., KALABUKHOV S., SHNECK R., ZARETSKY E., FRAGE N., *J. Eur. Ceram. Soc.*, 37 (2017), 3417.
[20] GHOSH A., DAS S.K., BISWAS J.R., TRIPATHI H.S., BANERJEE G., *Ceram. Int.*, 26 (2000), 605.
[21] HANAMURA E., KAWABE Y., TAKASHIMA H., SATO T., TOMITA A., *J. Nonlinear Opt. Phys. Mater.*, 12 (2003), 467.
[22] JOUNINI A., YOSHIKAWA A., BREINER A., FUKUDA T., BOULON G., *Phys. Stat. Sol. C*, 4 (2007), 1380.
[23] ZHANG Y., HUANG H., ZHANG K., DU S., YANG Y., WEN M., *Vacuum*, 146 (2017), 11.
[24] CULLITY B.D., *Elements of X-ray diffraction*, Addison-Wesley Publishing Company, Massachusetts, 1978.
[25] KAYGILI O., KESER S., TATAR C., KOYTEPE S., ATES T., *J. Therm. Anal. Calorim.*, 128 (2017), 765.
[26] KAYGILI O., KESER S., *Mater Lett.*, 141 (2015), 161.
[27] SABERI A., GOLESTANI-FARD F., SARPOOLAKY H., WILLERT-PORADA M., GERDES T., SIMON R., *J. Alloy. Compd.*, 462 (2008), 142.
[28] SANJABI S., OBEYDAVI A., *J. Alloy. Compd.*, 645 (2015), 535.
[29] DERAZ N.M., ABD-ELKADER O.H., *Int. J. Electrochem. Sci.*, 8 (2013), 8632.
[30] MADHURI W., ROOPAS KIRAN S., PENCHAL REDDY M., RAMAMANOHAR REDDY N., SIVA KUMAR K.V., *Mater. Sci.-Poland*, 35 (2017), 44.
[31] KUTTY P.V.M., DASGUPTA S., *Ceram. Inter.*, 39 (2013), 7891.
[32] MOSAYEBI Z., REZAEI M., HADIAN N., KORDSHULI F.Z., MESHKANI F., *Mater. Res. Bull.*, 47 (2012), 2154.
[33] PEI L.Z., YIN W.Y., WANG J.F., CHEN J., FAN C.G., ZHANG Q.F., *Mat. Res.*, 13 (2010), 339.
[34] EWAIS E.M.M., BESISA D.H.A., EL-AMIR A.A.M., EL-SHEIKH S.M., RAYAN D.E., *J. Alloy. Compd.*, 649 (2015), 159.
[35] GUSMANO G., NUNZIANTE P., TRAVERSA E., *J. Eur. Ceram. Soc.*, 7 (1991), 31.
[36] EWAIS E.M.M., EL-AMIR A.A.M., BESISA D.H.A., ESMAT M., EL-ANADOULI B.E.H., *J. Alloy. Compd.*, 691 (2017), 822.
[37] ALVAR E.N, REZAEI M., ALVAR H.N., FEYZALLAHZADEH H., YAN Z.F., *Chem. Eng. Commun.*, 196 (2009), 1417.

Received 2018-07-18
Accepted 2019-03-07